JOURNAL OF MATERIALS SCIENCE **35** (2000) 567–572

The determination of the elastic modulus of microcantilever beams using atomic force microscopy

B. T. COMELLA*, M. R. SCANLON
Department of Mechanical Engineering, Rochester Institute of Technology, Rochester, NY, 14623
E-mail: comella@buffalo.edu

An investigation into the determination of the micromechanical properties of thin film materials has been performed. Thin metal and ceramic films are used extensively in the computer microprocessor industry and in the field of micro-electromechanical systems (MEMS). The demand for miniaturization and increased performance has resulted in the use of materials without a clear understanding of their mechanical properties on this scale. Micromechanical properties are difficult to obtain due to the lack of adequate testing equipment. The atomic force microscope (AFM), most commonly used as an imaging tool, lends itself to mechanical interaction with the sample surface utilizing a cantilever probe. An array of aluminum microcantilever beams were fabricated using standard IC processing techniques. The microbeams were deflected by the AFM cantilever probe and from this, the micromechanical properties of stiffness and elastic modulus were determined. Initial results indicate that this technique reliably determines the micromechanical properties of thin films.

1. Introduction

The growth of microfabrication process technologies and the development of micro-electromechanical systems (MEMS) increases the need for simple, reliable test methods to determine the mechanical properties of thin films. Miniaturization of computer microprocessors, and the development of MEMS utilize thin films a few angstroms to a few microns in thickness. Mechanical properties on this scale may differ from macroscale properties and as the MEMS structures get smaller the surface and size effects become increasingly important. Theory governing macroscale properties can scale down to provide explanation for experimental observation, however at some scale the macroscale theories break down.

Determining the mechanical properties of micro or nanoscale materials is a challenge due inadequate testing equipment. The testing equipment must be capable of applying loads on the order of 10^{-6} to 10^{-9} Newtons and measure deflections on the order of nanometers. Experimental methods developed to date include a capacitance/voltage measurement technique on fixed beam bridge structures [1], a technique to measure resonant frequency on a cantilever beam structure [2, 3], and deflection of cantilever beams [4].

Scanning probe microscopy (SPM) refers to a family of imaging instruments that use a profilometer to physically scan a surface. In this experiment a Dimension 3000 SPM manufactured by Digital Instruments was used for beam deflection experiments. Atomic force microscopy (AFM), one mode of the SPM, utilizes a cantilever/tip assembly to physically scan a sample while deflection information of this probe maps the surface. In addition to topographical imaging, the AFM lends itself to mechanical interaction with a sample surface and has recently been utilized to measure mechanical properties [5, 12].

In this project microfabrication techniques were used to create several microscale cantilever and simply supported beams with varying thickness, width, and length. The final material tested, common to most microfabrication facilities, was aluminum with 1% silicon. The AFM cantilever probe physically deflected the test beams while the pertinent deflection data was collected. The AFM cantilever was fabricated from silicon and is approximately 125 μm long and 5 μm thick. This cantilever was precisely controlled by a piezoelectric scanner tube which translates in all three dimensions by applying a voltage across its electrodes. A well built scanner can generate motion well below 1 angstrom.

The method developed used the fine control of the AFM cantilever to deflect the microbeams. The compilation of deflection data, elementary beam theory, and the geometry of the test structures determined the stiffness and elastic modulus of the thin film material.

* All correspondence should be to Brandon T. Comella, Dept. of Mech. and Aerospace Eng., 388 Lafayette Ave., Buffalo, NY 14213.

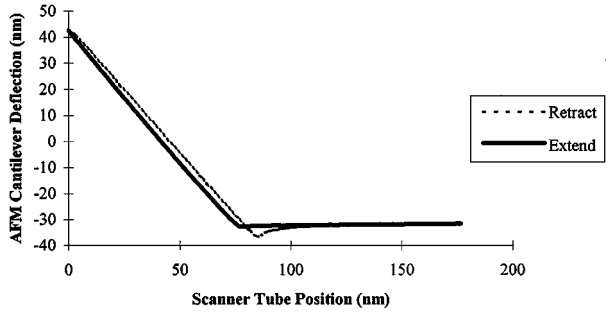

Figure 1 Force curve on diamond, 30 V.

2. Experimental theory

Applying a voltage to the piezoelectric scanner tube causes it to extend in a vertical direction, resulting in contact between the AFM cantilever and the sample surface. During this vertical extension, a force curve, as shown in Fig. 1, can be generated which is a plot of the AFM cantilever deflection versus the voltage applied to the piezo scanner tube. The data is primarily deflection data and force information is obtained only when the deflections are accurately calibrated and the spring constant of the AFM cantilever is determined. The spring constant is determined by adding end masses to the AFM cantilever and recording the change in resonant frequency [13].

Plotting the mass added versus $1/(2\pi f)^2$ where f is the resonant frequency of the AFM cantilever with the end mass, the slope of the resulting curve is the spring constant.

Calibration of the AFM cantilever deflection, Δz_t, versus piezo scanner tube extension, Δz_p, is necessary to obtain proper force relations. This is accomplished by first deflecting the AFM cantilever on an infinitely hard surface, such as diamond. The amount of AFM cantilever deflection is determined directly from the amount of piezo scanner tube extension. The relationship of the two deflections is obtained from the slope of the linear extending portion of the force curve as shown in Fig. 1. A correction is necessary for the angle of the AFM cantilever since it is mounted at 10 degrees below the horizontal. The result is

$$\Delta z_p = \Delta z_t \cos 10^\circ \tag{1}$$

where Δz_p is the piezo extension and Δz_t is the AFM cantilever deflection. The slope of the force curve, called the 'Sensitivity', is given by

$$S = \frac{\Delta z_t}{\Delta z_p} \tag{2}$$

Solving (1) to be of the form of (2) yields

$$S = \frac{1}{\cos 10^\circ} = 1.015 \tag{3}$$

on an infinitely hard surface. This quantity is the amount of voltage change in the position sensitive detector (PSD) for a known amount of scanner tube extension and has units of Volts/nm. Once the AFM cantilever deflection and spring constant are determined, the amount of force applied to the sample surface can be calculated using Hooke's Law.

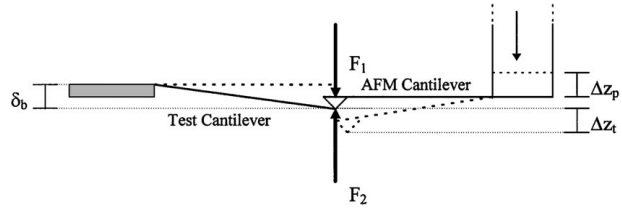

Figure 2 Schematic of AFM cantilever and test beam.

$$F = k_t \Delta z_t \tag{4}$$

where k_t is the spring constant of the AFM cantilever.

After the spring constant of the AFM cantilever is obtained, and the relationship between the AFM cantilever deflection and scanner tube extension is accomplished, the fabricated aluminum microbeams could then be deflected and the elastic modulus determined. In an experiment similar to that conducted by Torri *et al.* [14], the AFM cantilever is used to deflect the aluminum microbeams and the deflection of the AFM cantilever is monitored. To calculate the stiffness and elastic modulus, the following development, based on Newton's First Law, was used and will be referred to as the 'Differential Method'. The system consisting of two cantilevers are considered to be in static equilibrium at each instant.

In Fig. 2, F_1 is the force exerted by the AFM cantilever, F_2 is the equal and opposite force exerted by the aluminum microbeam. Δz_p, Δz_t and δ_b are the vertical deflections of the piezoelectric tube, the AFM cantilever and the aluminum microbeam, respectively. Observing Fig. 2, the two forces have to be equal to satisfy static equilibrium resulting in,

$$\sum F = F_1 - F_2 = 0 \tag{5}$$

Incorporating Hooke's Law into (5) yields

$$k_t \Delta z_t = k_b \delta_b \tag{6}$$

where k_t is the spring constant of the AFM cantilever and k_b is the stiffness of the microbeam. The total travel of the piezo scanner tube is given by

$$\Delta z_p = \delta_b + \Delta z_t \cos 10^\circ \tag{7}$$

where Δz_p is known and Δz_t is monitored by the AFM. Solving for δ_b results in

$$\delta_b = \delta z_p - \Delta z_t \cos 10^\circ \tag{8}$$

and substituting into (6) yields an equation with only one unknown quantity, k_b,

$$k_t \Delta z_t = k_b(\Delta z_p - \Delta z_t \cos 10^\circ). \tag{9}$$

With (9), the stiffness of the microbeam can be found if the actual deflections (Δz_p, Δz_t) are known. Assuming

infinitesimally small deflections and modifying (9) results in

$$k_t d\Delta z_t = k_b(d\Delta z_p - d\Delta z_t \cos 10^\circ). \qquad (10)$$

Dividing (10) by $d\Delta z_p$ and making the substitution,

$$S^* = \frac{d\Delta z_t}{d\Delta z_p}, \qquad (11)$$

which is the slope of the contact region of the force curve, results in the final form,

$$k_b = \frac{k_t S^*}{(1 - S^* \cos 10^\circ)}. \qquad (12)$$

In this form, to find the stiffness of the microbeam, the AFM cantilever stiffness must be known along with the slope of the force curve. Equation 12 accounts for all data pairs that lie along the contact portion of the force curve.

Once the microbeam stiffness is determined, elastic modulus is calculated using,

$$E_b = \frac{k_b L_b^3}{3\Gamma_z}. \qquad (13)$$

3. Microbeam fabrication

The aluminum microbeams were fabricated using standard surface micro-machining techniques.

A mask containing four different length cantilever beams (50 μm, 75 μm, 100 μm, and 125 μm) with varying widths (20 μm, 30 μm, and 40 μm) in each of 12 possible combinations was generated and subsequently patterned on a silicon wafer.

In the initial processing step, polyimide, was placed as a sacrificial layer between the silicon and the metal. Once the polyimide was cured, aluminum with 1% silicon was sputtered onto the polyimide layer. Using a stylus profilometer, the resulting film measured 2.1 microns in thickness.

The photoresist layer was patterned to the final beam geometry using the mask and photolithography and a wet chemical etch removed exposed aluminum.

Finally the photoresist and the polyimide were removed to free the microstructures. This was accomplished using a dry etch in an oxygen plasma until the microstructures were free standing.

The cross section of the processing steps are shown in Fig. 3. SEM micrographs of the final microbeam structures are shown in Figs 4 and 5.

4. Experimental

The spring constant of the silicon cantilever was determined using tungsten spheres, and the piezo was calibrated using diamond as an infinitely stiff material.

To deflect the microbeams, a continuous triangular voltage waveform was applied to the piezo scanner tube and the force curve was subsequently displayed. The vertical position of the force curve was adjusted by varying the setpoint. Horizontal adjustment was achieved by varying the z-scan start parameter which

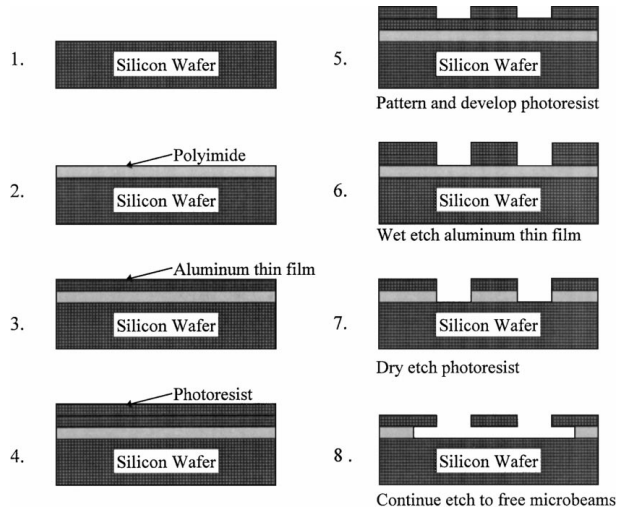

Figure 3 Cross section of the steps used to fabricate the free standing microstructures.

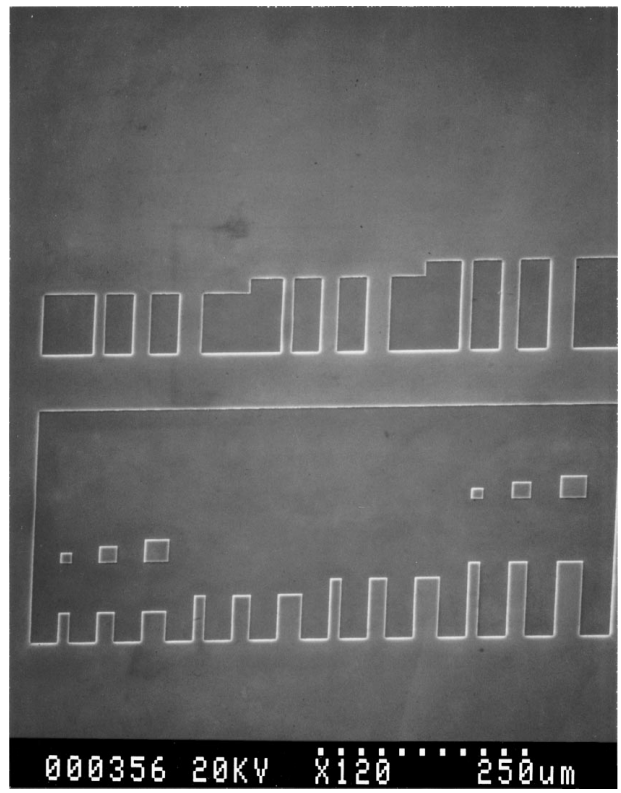

Figure 4 SEM micrograph of both cantilever and simply supported microbeams.

changed the relative position of the piezo scanner tube to the sample surface. Proper adjustments of the setpoint and z-scan start parameters were made until a curve similar to Fig. 1 was obtained.

From the force curve, the slope of the linear portion of the plot was determined by importing the data into Microsoft Excel and performing a least squares fit of the extending data as shown in Fig. 6. The original data imported did not represent the correct deflections and was transformed using equations obtained from Digital Instruments [15]. Sensitivity is a parameter that relates the PSD voltage to the piezo extension and upon testing on the diamond, the sensitivity was adjusted until the slope of the linear portion was equal to 1.015, as

Figure 5 SEM micrograph of cantilever microbeams.

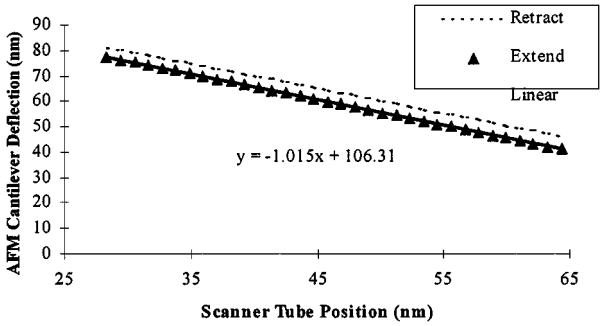

Figure 6 Linear portion of the calibration on the diamond.

determined in (3). At this point the PSD voltage versus piezo scanner tube extension is calibrated, and testing of the microbeams began.

Care was taken to ensure that the laser position and the z-scan size parameters were identical to those used in the calibration with the diamond sample. The z-scan size parameter controlled the size of the applied triangular waveform.

Cycling of the scanner tube commenced and the z-scan start and setpoint parameters were adjusted and the aluminum microbeam was deflected until the force curve was ideally located. The resulting force curve was then captured and analyzed as shown in Fig. 7.

An important observation is that the scanner tube extension along the horizontal axis in Fig. 7 was greater than the corresponding distance in Fig. 1. This confirms that, as expected, the scanner tube had to extend more to deflect the microbeams than it did to achieve the same AFM cantilever deflection on the diamond surface. It should noted that the actual extension of the piezo tube during the cycling did not change since the z-scan size

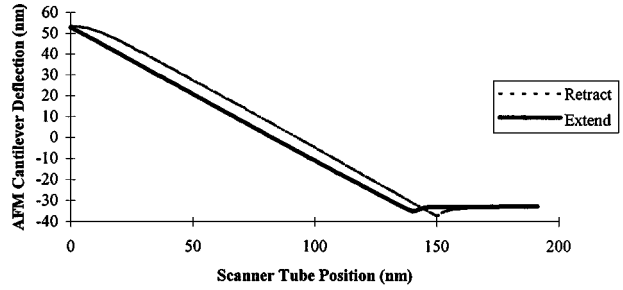

Figure 7 Force curve on microbeam, 30 V.

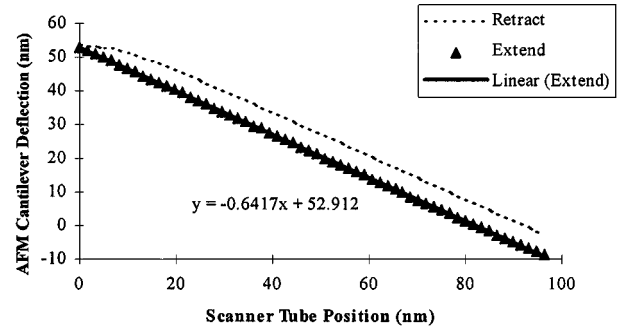

Figure 8 Linear portion of microbeam deflection, 30 V.

was constant. However, the z-scan start was adjusted manually until the AFM cantilever deflection was close to that in Fig. 1. It is the sum of the manual adjustment and the cycling voltage that accounts for the increased scanner tube extension in Fig. 7.

The slope of the linear portion of the piezo extension curve as shown in Fig. 8, along with the spring constant of the AFM cantilever was all that was needed to determine the stiffness according to the differential method developed earlier in (12).

5. Results

By attaching tungsten beads to the end of the silicon cantilever and measuring the subsequent change in the resonant frequency, the stiffness of the silicon AFM cantilever was determined to be $k_t = 77$ N/m.

The width of each aluminum microbeam tested was confirmed to be 20 μm and the thickness of the thin film was measured to be 2.1 μm. Several of the microbeams were selected for testing, at various z-scan size values. Changing the z-scan size parameter increases or decreases the amplitude of the triangular waveform and for a given beam length resulted in a change in the applied force, and therefore deflection of the microbeams.

The stiffness of the aluminum microbeams was determined using (12) and the results are summarized in Table I.

All of the aluminum microbeams had rectangular cross sections with a moment of inertia [16]

$$I_z' = 15.4\,\mu\text{m}^4.$$

Elastic modulus was computed using (13) and the results are summarized in Table II.

TABLE I Stiffness results for the aluminum cantilevers

z-Scan size (V)	Length (μm)	Slope on beam	Beam stiffness (N/m)
20	100	0.0424	3.41
20	100	0.0411	3.30
30	125	0.0252	1.99
40	125	0.0254	2.01
30	50	0.2505	25.74

TABLE II Elasticity results for aluminum microbeams

z-Scan size (V)	Length (μm)	Elasticity (MPa)
20	100	73628
20	100	71274
30	125	83961
40	125	84713
30	50	69471

6. Discussion

The experimental versus theoretical stiffness values of the deflected aluminum micro-cantilevers are summarized in Table III.

The experimental versus theoretical elasticity values are summarized in Table IV.

Two major sources of error can account for the deviation between experimental and theoretical values. The first is inaccuracy in the measurement of the spring constant of the silicon AFM cantilever. The technique employed relied on the attachment of small tungsten spheres to the end of the cantilever, and determination of the mass of these spheres from their geometry. Inaccuracies in the measurement of the geometry of the sphere resulted in errors in the value for the spring constant. The second source of error is the determination of the geometry of the aluminum microbeams, specifically the beam thickness. Elastic modulus is a function of the thickness to the third power and any error in the thickness measurement results in significant error in the modulus values.

TABLE III Experimental versus theoretical stiffness of aluminum microbeams

Length (μm)	Exp. stiffness (N/m)	Theor. stiffness (N/m)	% Deviation
50	25.74	25.93	1
100	3.30	3.24	2
100	3.41	3.24	5
125	2.01	1.66	21
125	1.99	1.66	20

TABLE IV Experimental versus theoretical elasticity values for aluminum microbeams

Length (μm)	Exp. relasticity (MPa)	Theor. elasticity (Mpa)	% Deviation
50	69471	69000	0.68
100	73628	69000	6.7
100	71274	69000	3.3
125	83961	69000	22
125	84713	69000	23

The variation of the results for a given length cantilever can be attributed to another source of error. If the AFM cantilever is not applied in the expected position along the length of the microbeam during the deflection process, then the value for L_b in (13) will be incorrect. For this experiment, this positioning process was done optically, and should be modified to be more precise.

7. Conclusions

A major limitation that has existed in the measurement of micromechanical properties of thin films is the scarcity of available equipment to measure properties on a micro scale. It has been demonstrated that the AFM is capable of applying micro or nano scale forces while monitoring the resulting deflections. It therefore lends itself as an appropriate instrument to determine micromechanical properties.

In structures microns or nanometers in size, surface and size effects become increasingly important. A major question exists as to whether the mechanical properties of a material on this scale are equivalent to macroscale values. The developed technique has proven to be an effective step towards answering this question. When sources of error present in this experiment are minimized, the values obtained from the deflection of microbeams can be directly compared to literature values for bulk materials. Any deviation from such values can be attributed to surface, size and scaling effects.

The method developed is applicable to beams of thickness ranging from angstroms to microns since the AFM is capable of applying small forces in a controlled environment. The use of the atomic force microscope along with the development of the differential method have proven to have great potential. With refinement this technique can be used to effectively determine the mechanical properties of nanoscale thin films.

References

1. S. WANG, S. CRARY and K. NAJAFI, *Mat. Res. Soc. Symp. Proc.* (1992) 203–208.
2. K. E. PETERSON, *IEEE Trans. Electron Devices* **ED-25**(10) (1978) 1241–1250.
3. H. A. C. TILMANS, PhD dissertation, MESA Research Inst., Univ. Twente, Enschede, The Netherlands, 1993.
4. J. A. SCWEITZ, *MRS Bulletin* (1992) 34–45.
5. N. A. BURNHAM, R. J. COLTON and H. M. POLLOCK, *J. Vac. Sci. and Tech. A* **9** (1991) 2548–2556.
6. S. M. HUES, R. J. COLTON, E. MEYER and H. J. GUNTHERODT, *MRS Bulletin* **18** (1993) 41–49.
7. N. A. BURNHAM and R. J. COLTON, *J. Vac. Sci. and Tech. A* **7** (1989) 2906–2913.
8. N. A. BURNHAM, R. J. COLTON and H. M. POLLOCK, *Nanotechnology* **4** (1993) 64–80.
9. S. M. HUES, C. F. DRAPER and R. J. COLTON, *J. Vac. Sci. and Tech. B* **12** (1994) 2211–2214.
10. M. R. VANLANDINGHAM, S. H. MCKNIGHT, G. R. PALMESE, R. F. EDULJEE, J. W. GILLESPIE, Jr. and R. L. MCCULLOGH, *J. Mater. Sci. Letters*, submitted, 1996.
11. M. R. VANLANDINGHAM, S. H. MCKNIGHT, G. R. PALMESE, J. R. ELINGS, X. HUANG, T. A. BOGETTI,

R. F. EDULJEE and J. W. GILLESPIE, Jr., *J. Adhesion*, submitted, 1996.
12. M. R. VANLANDINGHAM, S. H. MCKNIGHT, G. R. PALMESE, R. F. EDULJEE, J. W. GILLESPIE, Jr. and R. L. MCCULLOGH, *Mat. Res. Soc. Proc.* (1997) 440.
13. J. P. CLEVELAND, S. MANNE, D. BOCEK and P. K. HANSMA, *Rev. Sci. Instrum.* **64**(2) (1993) 403–405.
14. A TORII, M. SASAKI, K. HANE and S. OKUMA, *Meas. Sci. Tech.* **7** (1996) 179–184.
15. Digital Instruments, Santa Barbara, California.

Received 26 February
and accepted 16 August 1999